

The effect of Ti additions on the hydrogen absorption properties of mechanically alloyed Mg₂Ni powders

C.K. Lin^{a,*}, C.K. Wang^a, P.Y. Lee^b, H.C. Lin^c, K.M. Lin^a

^a Department of Materials Science and Engineering, Feng Chia University, Taichung 407, Taiwan, ROC

^b Institute of Materials Engineering, National Taiwan Ocean University, Keelung 202, Taiwan, ROC

^c Department of Materials Science and Engineering, National Taiwan University, Taipei 106, Taiwan, ROC

Received 23 August 2005; received in revised form 30 November 2005; accepted 15 February 2006

Abstract

In the present study, mechanical alloying technique was used to prepare (Mg₂Ni)_{100-x}Ti_x ($x=0, 2.5, 5, 7.5,$ and 10 wt.%) powders starting from elemental powder mixture under an Ar atmosphere. The experimental results showed that the absorbed hydrogen content and reversible hydrogen content was 3.14 and 2.40 wt.% for 15 h milled Mg₂Ni powders, respectively. The maximum hydrogen absorption content was increased to over 3.8 wt.% with Ti additions. The reversible hydrogen content also increased significantly (18–25%) with Ti additions. Meanwhile, 15 h milled Mg₂Ni–Ti powders can absorb more than 3 wt.% of hydrogen within 1000 s. Not only the hydrogen absorption ability but the hydrogen absorption rate were improved by the additions of titanium and MA treatment in Mg₂Ni alloy.

© 2006 Elsevier B.V. All rights reserved.

Keywords: Mechanical alloying; Hydrogen absorption; Mg₂Ni; X-ray absorption

1. Introduction

Considerable effort has been concentrated on the hydrogen technologies from the energy and environmental point of view. The major techniques for hydrogen storage include to develop compressed high-pressure gas cylinder, condensation into liquid or even solid hydrogen, hydrogen absorption on large-surface-area solids such as carbon nanotubes, and metal hydrides [1]. Among those, hydrogen storage by metal hydrides has attracted R&D interests due to the lighter weight, higher hydrogen absorption percentage, and relatively low cost. Metal hydrides can also be used in many other applications such as purification, hydride heat pump, transportation, nickel/metal hydride batteries, etc. [2,3].

Metal hydrides for hydrogen storage can be classified into various groups including AB, AB₂, A₂B, and AB₅ [4]. A₂B type Mg₂Ni with its high hydrogen content up to 3.6 wt.% is a potential candidate for practical application. The low hydriding/dehydriding rate, however, limits its practical application. Mechanical alloying (MA) process has been used successfully to

prepare metal hydrides [5–7]. By mechanically grinding starting materials, not only the grain size can be reduced but the defect concentration increases. Thus hydrogen absorption properties can be improved. For instance, Zaluski et al. [8] have improved the hydrogen absorption performance of Mg₂Ni by MA. In the present study, we intend to improve further the Mg₂Ni alloy by adding reactive Ti elements. MA technique was used to prepare Mg₂Ni–Ti alloy powders. The structure and hydrogen absorption properties of as-milled powders were investigated.

2. Experimental

Elemental powders of Mg (99.8%, <50 mesh), Ni (99.98%, <300 mesh) and Ti (99.7%, <100 mesh) were weighed to yield the desired compositions: (Mg₂Ni)_{100-x}Ti_x ($x=0, 2.5, 5, 7.5,$ and 10), and then canned into an SKH 9 high speed steel vial together with Cr steel balls (7 mm in diameter with ball-to-powder ratio = 5:1) under an argon-filled glove box, where a SPEX 8000D shaker ball mill was used for MA. The overall process lasted 15 h and were interrupted every 15 min for the first hour and every 30 min thereafter. Each interruption was followed by an equal length of time (~30 min.) to cool down the vials. The milling status was examined by using X-ray diffraction and synchrotron X-ray absorption techniques. The

* Corresponding author. Tel.: +886 4 24517250x5309; fax: +886 4 24510014.
E-mail address: cclin@fcu.edu.tw (C.K. Lin).

X-ray analysis was performed using a Siemens D-5000 diffractometer (Cu K α radiation). X-ray absorption spectroscopy measurements [9] were performed at the Wiggler-C beamline of the National Synchrotron Radiation Research Center (NSRRC) in Hsinchu, Taiwan. The hydrogen absorption properties of 15 h as-milled $(\text{Mg}_2\text{Ni})_{100-x}\text{Ti}_x$ powders were evaluated by pressure–composition–temperature (PCT) measurements, differential scanning calorimetry, and thermo-gravimetry analysis (SDT2960 Simultaneous DSC-TGA, TA Instrument). The PCT measurements were performed at 350 °C, while DSC/TGA measurements were performed under an Ar atmosphere at a heating rate of 5 °C/min.

3. Results and discussion

3.1. Structural characterization

Fig. 1a shows the X-ray diffraction patterns of the as-milled Mg_2Ni powders with various milling times. Crystalline Mg and Ni diffraction peaks were observed at the early stage of milling and the peak intensities decreased gradually with increasing milling time. Formation of Mg_2Ni phase can be noticed after 4 h of milling treatment. Mg_2Ni phase with Mg and Ni solid solutions were obtained after 5 h of MA processing. Grain size reduction and/or residual strain arose from the MA treatment induced observable peak broadening. It is also interesting to note that the relative amount of Mg_2Ni , Mg, and Ni phases varied with prolonged milling (compared the XRD patterns of 5, 10, and 15 h) [10]. The addition of Ti elements influences the structural evolution during MA. The formation of Mg_2Ni phase was delayed to a milling time of 5 h or more. For instance, the XRD patterns of as-milled $(\text{Mg}_2\text{Ni})_{95}\text{Ti}_5$ alloy powders was shown in Fig. 1b, where only limited Mg_2Ni peak can be observed after 5 h of milling treatment. A similar trend was observed at the other compositions (Ti = 2.5, 7.5 and 10 at.%). It was thought

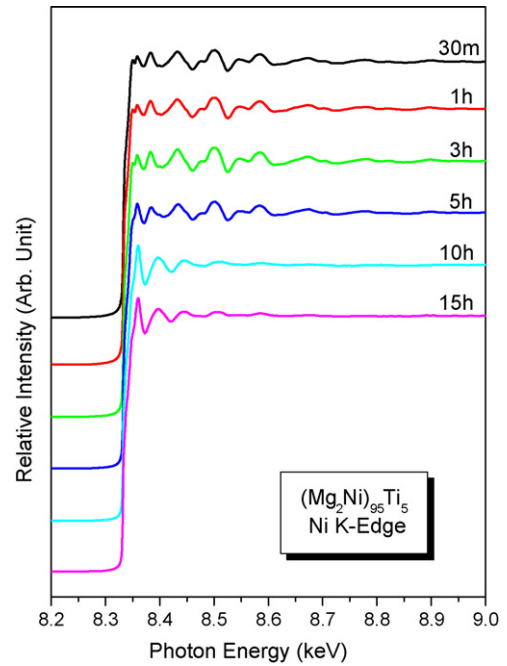


Fig. 2. Ni K edge absorption spectra for $(\text{Mg}_2\text{Ni})_{95}\text{Ti}_5$ powders with respect to the milling time.

that Ti elements were dissolved into Mg_2Ni matrix and the 15 h milled $(\text{Mg}_2\text{Ni})_{100-x}\text{Ti}_x$ alloy powders were consisted of different ratios of Mg_2Ni , Mg, and Ni solid solutions.

Except the long range order revealed by the X-ray diffraction technique, extended X-ray absorption fine structure (i.e., EXAFS) technique was used to investigate the local atomic change during MA. EXAFS spectra (Ni K edge, 8333 eV) of the as-milled $(\text{Mg}_2\text{Ni})_{95}\text{Ti}_5$ alloy powders as a function of milling time are shown in Fig. 2. Similar trend can be observed for as-milled Mg_2Ni powders. It can be noted that EXAFS spectra for those at the early stage of milling (up to 3 h of milling)

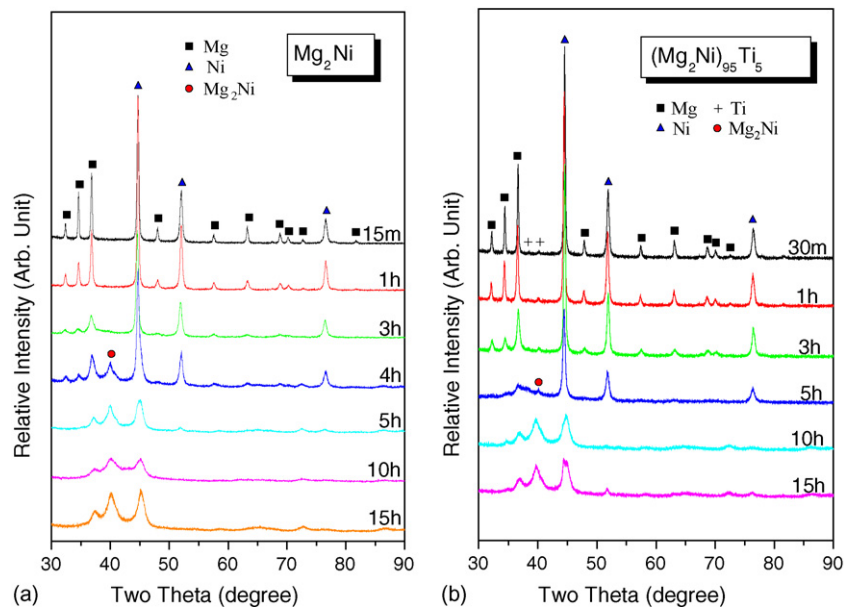


Fig. 1. X-ray diffraction patterns of (a) Mg_2Ni and (b) $(\text{Mg}_2\text{Ni})_{95}\text{Ti}_5$ powders as a function of milling time.

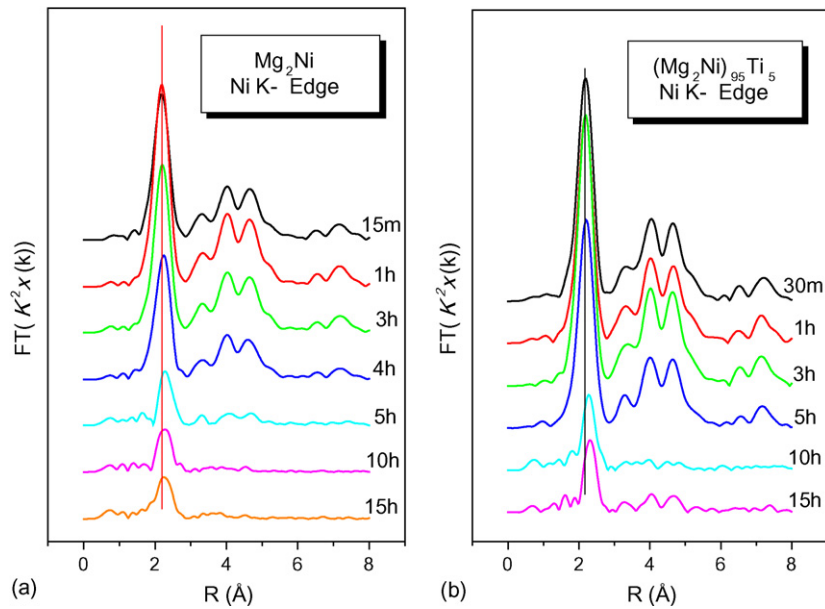


Fig. 3. Radial distribution functions for (a) Mg_2Ni and (b) $(\text{Mg}_2\text{Ni})_{95}\text{Ti}_5$ powders with milling time.

exhibited no significant change. The EXAFS spectrum of 10 h milled powders was different from that of 3 h one, while 5 h spectrum is the transient stage. The radial distribution function (RDF) of the local atomic environment of detected atom (i.e., Ni) can be determined after Fourier transformation [9]. Fig. 3 shows the RDFs for Mg_2Ni and $(\text{Mg}_2\text{Ni})_{95}\text{Ti}_5$ as-milled powders. The magnitudes of the RDF indicate the coordination numbers of detected atom at various distances. Similar RDFs can be observed at the early stage of milling (3 and 5 h for Mg_2Ni and $(\text{Mg}_2\text{Ni})_{95}\text{Ti}_5$, respectively). This indicates that the face-centered cubic structure of Ni persisted at the early stage of milling. Significant decrease in the high order peaks can be observed when the as-milled powders consisted of a mixture of Mg_2Ni , Mg, and Ni solid solutions, i.e., 5 and 10 h milling for Mg_2Ni and $(\text{Mg}_2\text{Ni})_{95}\text{Ti}_5$, respectively. A slight increase of the nearest neighbor bond-length can be noted and $(\text{Mg}_2\text{Ni})_{95}\text{Ti}_5$ powders exhibited a larger increase than that of Mg_2Ni powders. The addition of Ti elements not only postponed the formation of Mg_2Ni phase but expanded the nearest bond length of Ni.

X-ray absorption near edge structure (XANES) of Ti K edge for those of $(\text{Mg}_2\text{Ni})_{95}\text{Ti}_5$ powders was also investigated to reveal the electronic structure change during MA. Fig. 4 shows the XANES spectra of $(\text{Mg}_2\text{Ni})_{95}\text{Ti}_5$ as-milled powders. The pre-edge structure of Ti exhibited (the arrow in Fig. 4) at the early milling stage (before 5 h of milling). Slight difference for 5 h milled powders can be observed when compared with those milled less than 3 h. Pre-edge peak disappeared after 10 h milling. XANES spectra showed that Ti elements within the 5 h milled $(\text{Mg}_2\text{Ni})_{95}\text{Ti}_5$ powders persisted its electronic structure and changed with 10 h milling. Investigations by synchrotron X-ray absorption spectroscopy technique suggested that the $(\text{Mg}_2\text{Ni})_{95}\text{Ti}_5$ alloy powders exhibited elemental characteristics of Ni and Ti even after 5 h of milling treatment. While 5 h milled Mg_2Ni alloy powders, without Ti additions, exhibited a mixture of Mg_2Ni , Mg, and Ni solid solutions.

3.2. Hydrogen absorption properties

The PCT measurements of $(\text{Mg}_2\text{Ni})_{100-x}\text{Ti}_x$ milled powders for 15 h were performed at 350°C . As shown in Fig. 5a, the absorbed hydrogen content and reversible hydrogen content for Mg_2Ni 15 h milled powders was 3.14 and 2.40 wt.%, respectively. The hydrogen absorption properties can be improved significantly with the additions of Ti elements (only $(\text{Mg}_2\text{Ni})_{95}\text{Ti}_5$ was shown to avoid data overlap). The hydrogen content reached 3.84, 3.88, 3.82 and 3.81 with 2.5, 5, 7.5, and 10% Ti additions, respectively. Meanwhile, the reversible hydrogen content also

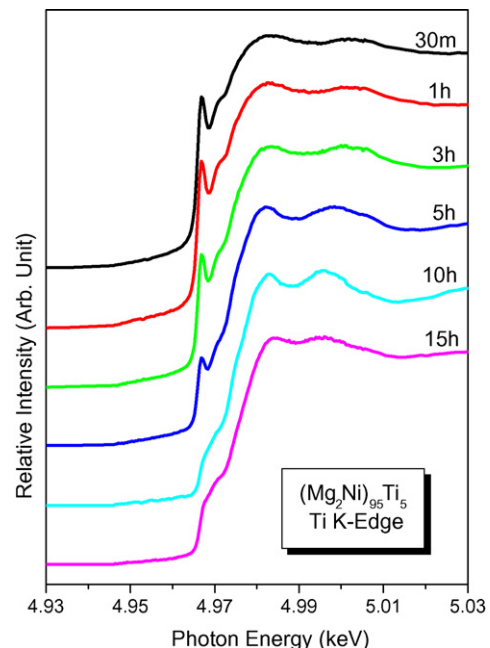


Fig. 4. Ti K edge absorption spectra for $(\text{Mg}_2\text{Ni})_{95}\text{Ti}_5$ powders with milling time.

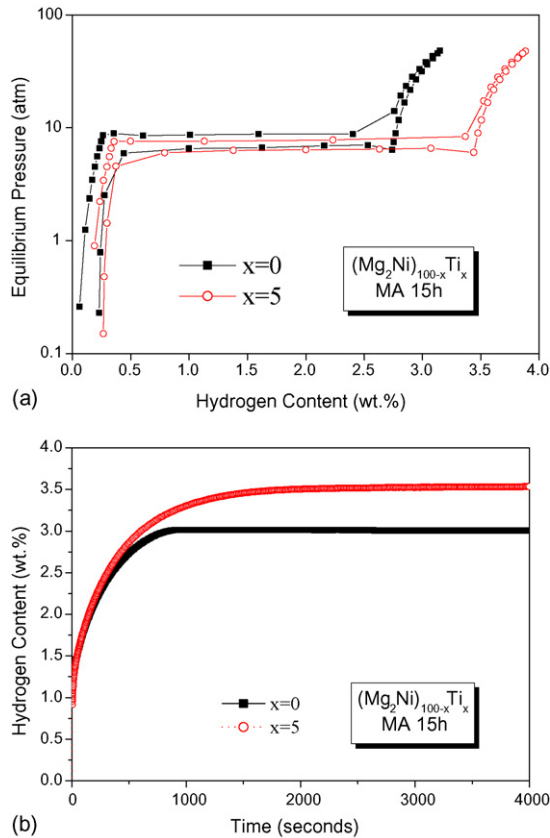


Fig. 5. (a) P–C–T and (b) kinetic curves for 15 h as-milled Mg_2Ni and $(Mg_2Ni)_{95}Ti_5$ powders.

increased (from 2.4 wt.% for Mg_2Ni) to 2.93, 3.01, 2.93, and 2.84 wt.%, respectively. It is suspected that the addition of Ti elements expanding the lattice structure may be attributed to the improvement of hydrogen absorption properties.

In Fig. 5a, it is also noted that the slope within the plateau region approached zero. Orimo et al. [11] have reported that this slope is related to the energy for hydrogen atom diffusion into the interstitial sites within the Mg_2Ni or Mg_2Ni –Ti lattices. Though MA process commonly induced high lattice strain, the hydriding at a temperature over 300 °C can eliminate the induced strain. The flat slope within the plateau region for 15 h as-milled Mg_2Ni –Ti powders indicated that hydrogen atom can diffuse into alloy powders without overwhelming a large energy barrier.

Fig. 5b shows the kinetic curves for 15 h as-milled Mg_2Ni –Ti powders. It can be noted that a significant improvement of hydrogen absorption can be observed with the Ti additions, similar to that revealed by Fig. 5a. For all the compositions investigated, 15 h as-milled Mg_2Ni –Ti powders can absorb more than 3 wt.% of hydrogen ($\sim 3.5\%$ with Ti additions) within 1000 s. This value is comparable to the value (3.4 wt.%) reported by Zaluski et al. [8] who also used MA technique to prepare nanocrystalline Mg_2Ni powders. The differences may be attributed to the MA processing and/or PCT testing parameters.

Fig. 6 shows the TGA/DSC curves of Mg_2Ni –Ti powders. Hydrided Mg_2Ni powders exhibited a dehydrating temperature of 220 °C, while no distinct dehydrating temperature can be

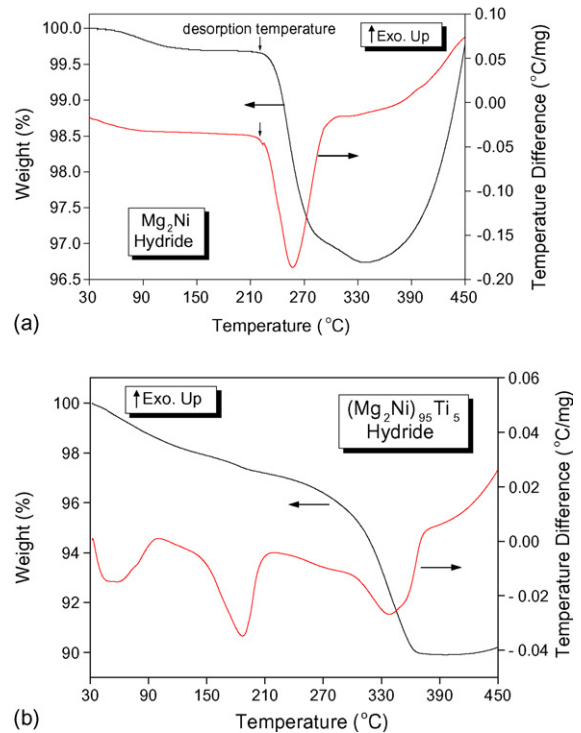


Fig. 6. TGA/DSC curves for hydrided (a) Mg_2Ni and (b) $(Mg_2Ni)_{95}Ti_5$ powders.

observed for $(Mg_2Ni)_{95}Ti_5$ powders. Though not shown here, hydrided $(Mg_2Ni)_{92.5}Ti_{7.5}$ and $(Mg_2Ni)_{90}Ti_{10}$ powders exhibited a dehydrating temperature of 203 and 243 °C, respectively. While with a limited Ti additions (2.5 or 5 at.%), dehydrating behavior occurred over a wide temperature range. Fujii et al. [12] have reported that, during the hydriding of mechanically alloyed powders, hydrogen atoms may occupy the interstitial sites and the intergranular defects. Dehydrating may occur between intra- and inter-grain regions. Therefore a decrease in the dehydrating temperature can be observed for mechanically alloyed powders [12].

In the present study, $(Mg_2Ni)_{92.5}Ti_{7.5}$ powders exhibited a maximum and reversible hydrogen content of 3.82 and 2.93 wt.%, respectively, while dehydrated at a relative low temperature of 203 °C. The overall hydrogen absorption properties can be improved with Ti additions.

4. Summary

Hydrogen absorption $(Mg_2Ni)_{100-x}Ti_x$ alloy powders were synthesized by mechanical alloying. The 15 h milled $(Mg_2Ni)_{100-x}Ti_x$ powders exhibited a mixture of Mg_2Ni , Mg, and Ni solid solutions. The 15 h milled Mg_2Ni powders exhibited a maximum and reversible hydrogen content of 3.14 and 2.40 wt.%, respectively. The maximum hydrogen absorption content increased from 3.14 wt.% to a value larger than 3.8 wt.% with Ti additions. Reversible hydrogen content improved from 2.40 wt.% for Mg_2Ni powders to 2.93, 3.01, 2.93, and 2.84 wt.% with 2.5, 5, 7.5, and 10% Ti additions, respectively. The dehydrating temperatures also decreased from 220 °C for Mg_2Ni to

203 °C for (Mg₂Ni)_{92.5}Ti_{7.5} powders. The additions of titanium and MA treatment did improve the hydrogen absorption properties of Mg₂Ni alloy.

Acknowledgements

This project was funded by Feng Chia University Distinguished Research Program (FCU-93GB27). The entire staff at NSRRC were also thanked.

References

- [1] J. Huot, in: H.S. Nalwa (Ed.), *Nanoclusters and Nanocrystals*, American Scientific Publishers, Stevenson Ranch, 2003, p. 53.
- [2] Q.D. Wang, C.P. Chen, Y.Q. Lei, *J. Alloys Compd.* 629 (1997) 253.
- [3] V. Güther, A. Otto, *J. Alloys Compd.* 889 (1999) 293.
- [4] L. Schlapbach, A. Züttel, *Nature* 414 (2001) 23.
- [5] C. Suryanarayana, *Int. Mater. Rev.* 40 (1995) 41.
- [6] M. Abdellaoui, D. Cracco, A. Percheron-Guegan, *J. Alloys Compd.* 293–295 (1999) 501.
- [7] R. Schulz, J. Huot, G. Liang, S. Boily, G. Lalande, M.C. Denis, J.P. Dodelet, *Mater. Sci. Eng. A* 267 (1999) 240.
- [8] L. Zaluski, A. Zaluski, J.O. Ström-Olsen, *J. Alloys Compd.* 217 (1995) 245.
- [9] C.K. Lin, P.Y. Lee, J.L. Yang, C.Y. Tung, N.F. Cheng, Y. Hwu, *J. Non-Cryst. Solids* 232–234 (1998) 520.
- [10] L. Aymard, M. Ichitsubo, K. Uchida, E. Sekreta, F. Ikazaki, *J. Alloys Compd.* 259 (1997) L5.
- [11] S. Orimo, H. Fujii, *Appl. Phys. A* 72 (2001) 167.
- [12] H. Fujii, S. Orimo, K. Ikeda, *J. Alloys Compd.* 253–254 (1999) 80.